# Total energies in Se. I. The trigonal crystal

David Vanderbilt
*Department of Physics, University of California at Berkeley, Berkeley, California 94720*

J. D. Joannopoulos
*Department of Physics, Massachusetts Institute of Technology, Cambridge, Massachusetts 02139*

(Received 7 September 1982)

The equilibrium crystal structure (lattice constants and chain radius) of trigonal selenium, a molecular crystal, are determined by minimizing the total energy, as calculated in the local-density and frozen-core approximations. The cohesive energy and $\Gamma_1(A_1)$ phonon frequency are also computed. Comparison with experiment shows excellent agreement for intrachain properties, and satisfactory agreement for interchain properties. This indicates that *ab initio* local-density total-energy calculations are viable for the case of molecular crystals.

## I. INTRODUCTION

The development of accurate *ab initio* pseudopotentials[1–5] has made it possible to perform realistic calculations of total energies within the local-density approximation[6] for covalently bonded semiconductors[7–11] and metals.[12–14] Here we present the first application of these techniques to a molecular crystal. We consider trigonal selenium, which consists of infinite helical chains of covalently bonded atoms. Because of the weak interchain bonding, sometimes ascribed to van der Waals forces, this system provides a particularly stringent test case for a local-density theory of total energies.

We begin with a discussion of the choice of pseudopotential in Sec. II. Section III contains a description of the calculations. In particular, the implementation of Löwdin perturbation theory[15] for total-energy calculations is discussed. In Sec. IV, we present and discuss the results for Se, and compare with experiment. Finally, in Sec. V we summarize briefly.

## II. CHOICE OF PSEUDOPOTENTIAL

In order to obtain accurate total energies, a pseudopotential is desired which accurately reproduces not only the eigenvalues, but also the wave functions outside the core region when compared with the all-electron case. An attempt at constructing such potentials was first made by Starkloff and Joannopoulos[1] (SJ) for local pseudopotentials. Their pseudo-wave-function could match the all-electron wave function outside the core to better than 1%. Recently, it has been pointed out that the pseudo- and real-wave-functions could be required to match exactly outside the core, if nonlocal pseudopotentials are used. In either case, the transferability of the pseudopotential is improved, because it can be proven that the energy derivatives of the phase shifts remain unchanged if the wave functions match.[3]

Various ways of constructing nonlocal pseudopotentials have now been proposed.[2–5] These potentials are of the form

$$\hat{U}_{\rm ps}(r)=\sum_l U_{{\rm ps},l}(r)\hat{P}_l \ . \tag{1}$$

For calculations done in a plane-wave basis, a soft core pseudopotential is desirable. The pseudopotential of Hamann, Schluter, and Chiang[3] (HSC) is of this type.

The use of a nonlocal potential, Eq. (1), introduces several inconveniences. For example, it becomes cumbersome to calculate gradients of the eigenvalues in $\vec{k}$ space, or to do $\vec{k}\cdot\vec{p}$ perturbation theory. Also, force calculations require an extra double sum.[16] While these disadvantages are not compelling, it would be useful if an accurate *local* pseudopotential was available.

The local SJ pseudopotential proposed for Se is of the form

$$U_{\rm ps}(r)=-f(r;\lambda,r_c)\frac{Z}{r} \ , \tag{2a}$$

$$f(r;\lambda,r_c)=\frac{1-e^{-\lambda r}}{1+e^{-\lambda(r-r_c)}} \ . \tag{2b}$$

In Fig. 1, we compare the local SJ pseudopotential (with $\lambda=10.196$ a.u.$^{-1}$, $r_c=0.922\,78$ a.u. with the HSC nonlocal pseudopotential [in the configuration

 

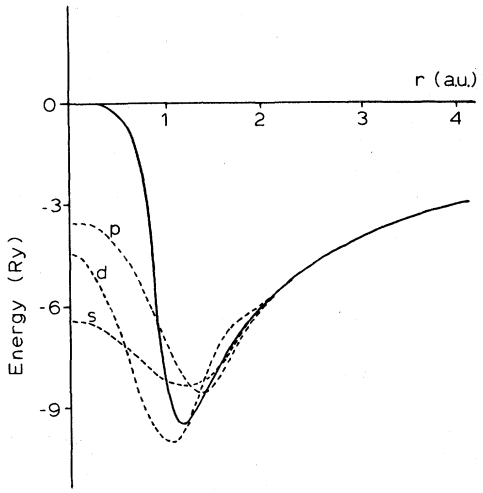


FIG. 1. Ionic pseudopotentials for Se. Solid line: local SJ potential (Ref. 4). Dashed lines: nonlocal HSC potential (Ref. 1).

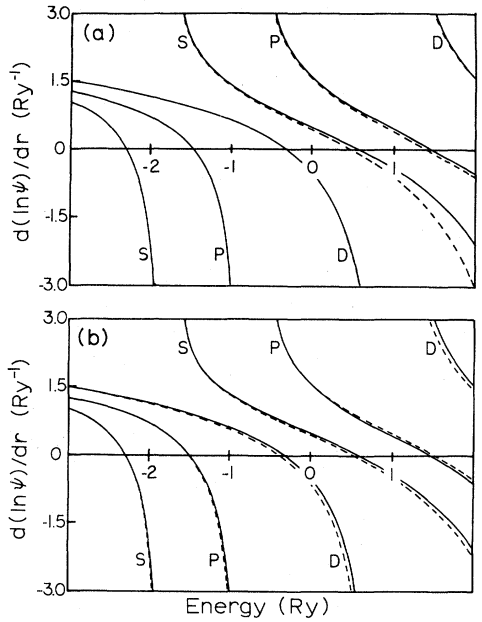


FIG. 2. Logarithmic derivatives of valence wave functions of Se vs energy at $R=3$ a.u. (a) Nonlocal HSC potential (Ref. 1). (b) Local SJ potential (Ref. 4). Solid lines are for all-electron wave functions; dashed lines are for pseudo-wave-functions.

$s^2p^{2.5}d^{0.5}$ with $r_c(s)=1.18$ a.u., $r_c(p)=1.24$ a.u., and $r_c(d)=1.18$ a.u.]. Both potentials were constructed using the Wigner form[17] for exchange correlation. Both potentials reproduce the $s$ and $p$ valence all-electron eigenvalues exactly. The SJ potential is constructed in such a way as to satisfy the norm-conserving property as well as possible. In fact, we find that the pseudo-wave-function and all-electron wave function differ by only $-0.14\%$ and $0.44\%$ for $s$ and $p$ waves, respectively, in the tail region. Thus norm conservation is obtained to an excellent approximation.

We further check the transferability of each potential by plotting the logarithmic derivative of the wave functions as a function of energy at a given radius. This is shown in Fig. 2. The HSC pseudopotential appears to do only slightly better than the SJ potential in this regard.

Thus the accuracy of the local SJ pseudopotential for Se is quite adequate. Its main drawback is the fact that the cutoff near $r_c$ must be substantially sharper than for the nonlocal potential. Consequently, more high Fourier components are required to represent the potential. For a plane-wave basis calculation, this implies that a larger matrix must be diagonalized to obtain the same accuracy. For this reason, we have chosen to work with the nonlocal HSC pseudopotential in the total-energy calculations presented here.

## III. BULK CALCULATIONS

The calculation of the total energy for the Se crystal is based upon the momentum-space formalism outlined by Ihm, Zunger and Cohen.[16] In addition, however, we have implemented the Löwdin perturbation scheme[15] as a way of reducing the size of the Hamiltonian matrix which must be diagonalized. When applied correctly, this allows a very substantial savings in computer time. Since the Löwdin scheme is not widely utilized in total-energy calculations, perhaps a few words are in order.

The Löwdin scheme reduces the size of the matrix to be diagonalized by including some higher Fourier basis vectors in first-order perturbation theory. Let roman letters label plane waves in set $A$ with energy $0<\epsilon_n<E_A$, and greek letters label plane waves in set $B$ with $E_A<\epsilon_\alpha<E_B$. Then we construct a renormalized Hamiltonian for set $A$ which includes set $B$ in perturbation theory:

$$U_{mn}=H_{mn}+\sum_{\alpha}\frac{H_{m\alpha}H_{\alpha n}}{\epsilon-\epsilon_\alpha}\ . \tag{3}$$

This is sometimes called "folding in" of the higher-energy components. The new Hamiltonian $U_{mn}$ has more accurate eigenvalues than $H_{mn}$.

Once $U_{mn}$ has been diagonalized, the eigenfunctions must be constructed in order to obtain the charge densities for the next self-consistent iteration. On one hand, it is possible to simply use the eigen-

states of $U_{mn}$ (that is, the wave functions have no Fourier components in set $B$). On the other hand, it is better to use the perturbed wave functions. If $\psi^\circ=\sum_n c_n\phi_n$ is the eigenvector, $U\psi^\circ=\epsilon\psi^\circ$, then the perturbed $\psi$ is

$$\psi=\psi^\circ+\sum_\alpha\left[\sum_n\frac{U_{\alpha n}}{\epsilon-\epsilon_\alpha}c_n\right]\phi_\alpha\ . \tag{4}$$

While the latter procedure (sometimes called "folding out" the wave function) is indeed preferable, it substantially increases the computer time required to compute and Fourier transform the charge densities. In practice, we find that if $E_A$ and $E_B$ are chosen large enough to be close to convergence (i.e., the cohesive energy is within $\sim 1$ eV/atom of the converged value), the folding-out procedure provides very little improvement in the total energy ($\sim 0.05$ eV/atom), although the charge densities are indeed substantially better. On the other hand, if $E_A$ is low enough, the folding out does substantially improve the total energy.

In the denominator of Eq. (3), it is necessary to replace the energy $\epsilon$ by some representative or average value $\bar{\epsilon}$. For band-structure or optical calculations, it is often customary to set $\bar{\epsilon}$ at or near the Fermi level, to give a good description of the gap. However, for ground-state total-energy calculations it is important to set $\bar{\epsilon}$ at the center of gravity of the filled valence levels (well below $\epsilon_F$). Otherwise, the energy denominator is systematically too small, so that the resulting eigenvalues and total energies are systematically too deep. We find that the correct choice of $\bar{\epsilon}$ substantially improves the effectiveness of the Löwdin method in reducing the cost of total-energy calculations.

To test the usefulness of the Löwdin perturbation scheme, we have carried out tests on the well-studied system of crystalline Si. The results are shown in Table I. It is seen that the Löwdin theory gives equally accurate results while allowing the cost of the calculation to be cut in half (compare cases 4–6). Case 3 is an actual 10-$\vec{k}$-point calculation identical to that of Yin and Cohen,[7] and it is gratifying that we reproduce their value to within $\sim 0.01$ eV. Using the Löwdin scheme, we can now go to more complete convergence. Cases 6–9 show that this adds $\sim 0.2$ eV to the theoretical binding energy. This worsens the agreement with experiment, but is consistent with the observation that cohesive energies calculated in local-density theory are generally too deep by several tenths of an eV.

In order to calculate the cohesive energy of Se, it is necessary to find the equilibrium structure by minimizing the energy with respect to structural degrees of freedom. The trigonal crystal structure of Se, shown in Fig. 3, has three degrees of freedom, which we take to be the first-neighbor distance $d_1$, the intrachain bond angle $\theta$, and the second-neighbor distance $d_2$ determining the interchain spacing.

The equilibrium geometry was determined as follows. First, $d_2$ was fixed at the experimental value of 3.42 Å.[18] Then $d_1$ and $\theta$ were varied in incre-

TABLE I. Tests for the convergence of the cohesive energy with respect to basis size for Si at the experimental lattice constant. Calculations were done at one $\vec{k}$ point, scaled to ten $\vec{k}$ points, and then corrected by a contant for zero-point motion and spin polarization. Wave functions were folded out whenever Löwdin perturbation sets were used. When values are not given for $E_B$, Löwdin perturbation was not used. Relative computer time per iteration per $\vec{k}$ point is shown in the last column.

| Case | $E_A$ (Ry) | $E_B$ (Ry) | $E_{\text{tot}}$ (eV/atom) | Time (sec) |
|---|---|---|---|---|
| 1 | 7.5 | | 3.95 | 21 |
| 2 | 9.5 | | 4.46 | 37 |
| 3 | 11.5 | | 4.68 | 64 |
| 4 | 7.5 | 11.5 | 4.70 | 30 |
| 5 | 9.5 | 11.5 | 4.68 | 42 |
| 6 | 11.5 | | 4.68 | 64 |
| 7 | 11.5 | 15.0 | 4.83 | 85 |
| 8 | 11.5 | 20.0 | 4.86 | 120 |
| 9 | 11.5 | 25.0 | 4.89 | 160 |

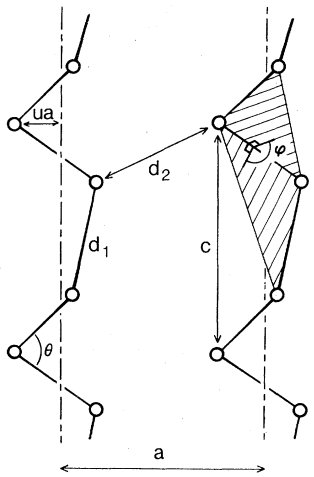


FIG. 3. Chain structure of trigonal Se, showing definitions of various structural parameters. Chains form a triangular lattice when viewed from the $c$ direction; only two chains are shown.

ments of 10% and 5° from the experimental values of 2.39 Å and 102.4°, respectively.[18] For each value of $d_1$ and $\theta$, the total energy was calculated using $E_A=3.48$ Ry and $E_B=11.60$ Ry, with the wave functions folded out, and with three special $k$ points[19] in the irreducible Brillouin zone. The two-dimensional matrix of total-energy values was fit by least squares to a third-order polynomial in $d_1$ and $\theta$. The parameters $d_1$ and $\theta$ were then held fixed at the values which minimized this polynomial while $d_2$ was varied in increments of 10%. The value of $d_2$ was obtained by fitting to a cubic polynomial and finding the minimum. With this new value of $d_2$ fixed, $d_1$ and $\theta$ were again varied as before to obtain their final values.

With the equilibrium geometry thus specified, the frequency of the $\Gamma_1$ ($A_1$) phonon frequency at zone center, corresponding to a breathing mode of the chains, was calculated in the frozen-phonon approximation by holding the two lattice constants $a$ and $c$ fixed and calculating the total energy for a series of values of the reduced chain radius $u$ (for notation see Fig. 3). Again a cubic fit to these results was performed to give the second derivative of the energy with respect to $u$. Finally, $E_A$ and $E_B$ were increased (up to 8.91 and 20.15 Ry, respectively) until we were confident that the cohesive energy was well converged with respect to basis set size. This resulted in an additional lowering of the cohesive energy by $\sim 1$ eV/atom. The effects of increasing the number of special $\vec{k}$ points was also checked, but was found to be negligible ($\sim 0.03$ eV/atom). Finally, the cohesive energy was calculated by subtracting off the energy of the pseudoatom, with a spin-polarization correction of 0.76 eV/atom, calculated by using the Hedin-Lundquist correlation.[20] For completeness, an estimate of the zero-point energy of the lattice was also included, although it amounts to only $\sim 0.02$ eV/atom in Se.

## IV. RESULTS AND DISCUSSION

Table II summarizes our results for the equilibrium geometry, cohesive energy, and $\Gamma_1$ ($A_1$) phonon frequency for trigonal Se. We find that the intrachain parameters $d_1$ and $\theta$ are in excellent agreement with experiment. The interchain distance $d_2$, on the other hand, is $\sim 10\%$ too short. The dependence of $E_{\text{tot}}$ on $d_2$ is illustrated in Fig. 4. Note the large anharmonicity, indicating that it is easier to stretch a bond than to compress it. The agreement for $d_2$ is felt to be quite reasonable in light of the difficulties in modeling the weak intermolecular binding of a molecular crystal. Evidently the local-density approximation is overestimating the strength of this binding.

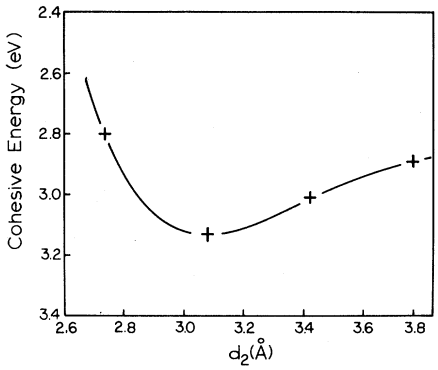


FIG. 4. Total energy of trigonal Se as a function of second-neighbor (interchain) distance $d_2$, with intrachain parameters ($d_1$ and $\theta$) held constant. Symbols show calculated points; solid curve is a guide to the eye.

Our calculated cohesive energy is found to be $\sim 1$ eV too deep compared to experiment.[21] Several factors probably contribute to this error. First, as mentioned in Sec. III, an overestimate of the cohesive energy by several tenths of an eV seems to be a general feature of local-density total-energy calculations. This could be due to an inaccurate description of the tail region of the free atom, or to some inadequacy in the description of electron correlations in the solid. In either case the error might be expected to be larger for a column-VI element simply due to the larger number of valence electrons. Second, the overestimate of the interchain binding undoubtedly plays a part. Third, omission of relativistic effects may introduce a small error. For most applications, an absolute error in the cohesive

TABLE II. Calculated minimum energy structure, cohesive energy, and $\Gamma_1$ ($A_1$) phonon frequency of trigonal Se, compared to experiment (Refs. 18 and 21). The notation is that of Fig. 3; in addition, $\phi$ is the dihedral angle along a chain, $E_{\text{coh}}$ is the cohesive energy per atom, and $\omega_{\text{ph}}$ is the frequency of the $\Gamma_1$ ($A_1$) phonon mode.

| | $d_1$ (Å) | $d_2$ (Å) | $\theta$ (deg) | $a$ (Å) | $c$ (Å) | $u$ | $\phi$ (deg) | $E_{\text{coh}}$ (eV) | $\omega_{\text{ph}}$ ($\text{cm}^{-1}$) |
|---|---|---|---|---|---|---|---|---|---|
| Theory | 2.367 | 3.104 | 102.60 | 3.974 | 4.913 | 0.2483 | 100.32 | 3.13 | 206 |
| Experiment | 2.390 | 3.422 | 102.48 | 4.366 | 4.955 | 0.2285 | 100.24 | 2.25 | 235 |

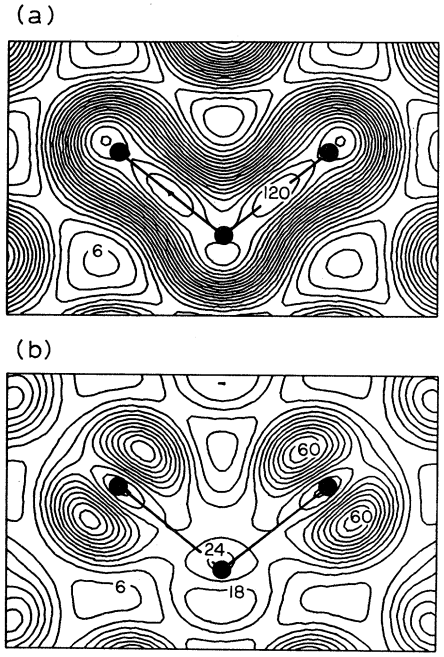


FIG. 5. Valence charge density of trigonal Se. (a) Sum of $s$ and $p$ bonding bands. (b) $p$ lone-pair band. The plane of the plot passes through three consecutive atoms (black dots) along the chain.

energy is not important as long as the total energy differences between two similar structures are well reproduced. The excellent agreement for $d_1$ and $\theta$ attest that this is the case. The agreement for the phonon frequency is also quite adequate.

The crystal has a calculated indirect gap from $M$ to $H$ of 0.7 eV, compared to the experimental value of 1.86 eV. That the gap is much too small is, of course, a general feature of local-density calculations, particularly when they are optimized to total energies rather than excitation properties (see, e.g., Ref. 7).

The calculated charge densities for the equilibrium structure are shown in Fig. 5. The charge density of the nonbonding (lone pair) orbitals has been plotted separately from that of the bonding orbitals for clarity. The intrachain bonding dominates, and there is no sign of strong covalent interchain bonding.

## V. SUMMARY

We have calculated the crystal structure and cohesive energy of trigonal Se within the local-density and frozen-core approximations. The intrachain structure is found to be very accurately reproduced. The interchain distance is given less accurately, as must be expected for a molecular crystal. However, the important features of trigonal Se, e.g., the strong asymmetry between strong intrachain and weak interchain bonding, are preserved intact. Thus we feel that the viability of local-density total-energy calculations for molecular crystals has been demonstrated.

## ACKNOWLEDGMENTS

This work was supported through the MIT Center for Materials Science and Engineering via National Science Foundation (NSF) Grant No. DMR-76-80895. Additional University of California (Berkeley) support in the latter stages of the work was provided by NSF Grant No. DMR-78-22465 and by the Director, Office of Energy Research, Office of Basic Energy Sciences, Materials Sciences Division of the U. S. Department of Energy under Contract No. DE-AC03-76SF00098. The authors (D.V. and J.D.J.) should also like to thank the Miller Institute and the John S. Guggenheim Foundation, respectively, for receipt of fellowships.

[1]Th. Starkloff and J. D. Joannopoulos, J. Chem. Phys. 68, 5794 (1978).
[2]A. Redondo, W. A. Goddard, III, and T. C. McGill, Phys. Rev. B 15, 5038 (1977).
[3]D. R. Hamann, M. Schluter, and C. Chiang, Phys. Rev. Lett. 43, 1494 (1979).
[4]A. Zunger and M. L. Cohen, Phys. Rev. B 20, 4082 (1979).
[5]G. Kerker, J. Phys. C 13, L189 (1980).
[6]P. Hohenberg and W. Kohn, Phys. Rev. 136, B864 (1964); W. Kohn and L. J. Sham, *ibid.* 140, A1133 (1965).
[7]M. T. Yin and M. L. Cohen, Phys. Rev. Lett. 45, 1004 (1980).
[8]A. Zunger, Phys. Rev. B 21, 4785 (1980).
[9]M. T. Yin and M. L. Cohen, Solid State Commun. 38, 625 (1981).
[10]J. Ihm and M. L. Cohen, Phys. Rev. B 23, 1576 (1981).
[11]J. Ihm and J. D. Joannopoulos, Phys. Rev. B 24, 4191 (1981).
[12]A. Zunger and M. L. Cohen, Phys. Rev. B 19, 568 (1979).
[13]P. K. Lam and M. L. Cohen, Phys. Rev. B 24, 4224 (1981).
[14]M. Y. Chou, P. K. Lam, and M. L. Cohen, Solid State Commun. 42, 861 (1982).
[15]P. Löwdin, J. Chem. Phys. 19, 1396 (1951).
[16]J. Ihm, A. Zunger, and M. L. Cohen, J. Phys. C 12,

4409 (1979).
[17]E. P. Wigner, Phys. Rev. 46, 1002 (1934).
[18]D. R. McCann and L. Cartz, J. Appl. Phys. 43, 4473 (1972); W. Lingelbach, J. Stuke, G. Weiser, and J. Treusch, Phys. Rev. B 5, 243 (1972).
[19]J. D. Chadi and M. L. Cohen, Phys. Rev. B 8, 5747 (1973).
[20]L. Hedin and B. I. Lundquist, J. Phys. C 4, 2064 (1971).
[21]C. Kittel, *Introduction to Solid State Physics,* 5th ed. (Wiley, New York, 1976), p. 74.